Simultaneous State Estimation and Tire Model Learning for Autonomous Vehicle Applications

Woongsun Jeon, Ankush Chakrabarty, Ali Zemouche and Rajesh Rajamani

***Abstract*— This paper addresses the problem of state estimation and simultaneous learning of the vehicle's tire model on autonomous vehicles. The problem is motivated by the fact that lateral distance measurements are typically available on modern vehicles while tire models are difficult to identify and also vary with time. Tire forces are modeled in the estimator using a neural network in which no a priori assumptions on the type of model need to be made. A neuro-adaptive observer that provides asymptotically stable estimation of the state vector and of the neural network weights is developed. The developed observer is evaluated using both MATLAB simulations with a low-order model as well as with an unknown high order model in the commercial software CarSim. Cornering and lane change maneuvers are used to learn the tire model over an adequately large range of slip angles. Performance with the low-order vehicle model is excellent with near-perfect estimation of states as well as the tire force nonlinear characteristics. Performance with the unknown high order CarSim model is also found to be good with the tire model being estimated correctly over the range of slip angles excited by the executed vehicle maneuvers. The developed technology can enable a new approach to obtaining tire models that are otherwise difficult to identify in practice and depend on empirical characterizations.**

***Index Terms*—Autonomous vehicles, neural networks, observers, tire force models, vehicle lateral dynamics.**

I. INTRODUCTION

THIS work is motivated by the fact that tire force models are most often represented empirically and are difficult to identify in practice. Linear models are often used and suffice for nominal non-aggressive operation on dry safe roads. However, nonlinear models become necessary when electronic stability control or other active safety systems need to be utilized, or in the case of slippery roads or aggressive maneuvers. Such nonlinear tire models are represented empirically using the Pacejka Magic Formula tire representation, the brush tire model or the Dugoff tire model [1]. The parameters of these imperfect models are difficult to identify in practice. Even in the case where a tire manufacturer has extensive test facilities to fully characterize and represent a tire, the real-world characteristics will vary with time due to both tire wear and also due to changes in pneumatic tire pressure.

This paper focuses on autonomous vehicles with automated steering for lane keeping. On such vehicles, the lateral distance with respect to the center of the lane and orientation with respect to the lane markers are measured and are used for automated steering, both to follow the lane and to perform automated lane changes during autonomous driving. The technical objectives in this paper are defined as real-time estimation of the state vector of the vehicle and simultaneous estimation of the tire force model of the vehicle. The tire force function is represented using a neural network and the weights of the neural network are identified in real-time. Unlike traditional neural networks, backpropagation is not utilized for training and no requirement to measure tire forces is necessary even for training the neural network. Instead, a neuro-adaptive observer is utilized to estimate both states and tire forces and the only measurements needed are the lateral feedback variables used in automated steering.

Previous researchers have developed a number of different vehicle state estimation methods while trying to use affordable sensors such as wheel speed sensors, IMUs, and GPS. In the development of these vehicle state estimation methods, various tire models are utilized. Lateral velocity estimation using state observers [2] and sideslip angle estimation using unknown input observer [3] have been developed based on linear tire models (tire force is linearly proportional to slip angle). Nonlinear observers [4], [5] have been developed for slip angle estimation based on the brush tire model. Slip angle estimation methods have also been developed by using the EKF [6], [7], UKF [8], and Fuzzy observers [9] based on the Dugoff tire model. Kalman filter-based methods (EKF, UKF, and Cubature Kalman filter) have been utilized for vehicle state estimation including lateral velocity [10] and slip angle estimation [11], [12] based on the Pacejka model. In all of these state estimation papers, the tire characteristics such as the tire model parameters and tire properties are assumed to be known.

For tire model identification, tire parameter estimation methods have been proposed [13] – [18]. Many researchers have focused on estimation of cornering stiffness for the linear tire model [13] - [16]. However, the linear tire model is

This research was funded in part by the US National Science Foundation, under grant PFI 1631133. Dr. Zemouche's time was supported in part by the ANR agency under the project ArtISMo ANR-20-CE48-0015.

Woongsun Jeon and Rajesh Rajamani are with the Department of Mechanical Engineering, University of Minnesota, Twin Cities, Minneapolis, MN 55455 USA (e-mail: jeonx121@umn.edu; rajamani@umn.edu).

Ankush Chakrabarty is with the Mitsubishi Electric Research Laboratories, Cambridge, MA 02139 USA (email: chakrabarty@merl.com).

Ali Zemouche is with the University of Lorraine, Lorraine 54400, France (email: ali.zemouche@univ-lorraine.fr).

applicable only under nominal driving conditions. Parameter estimation methods for nonlinear tire model structures have also been proposed based on the least squares method, but assume a known model structure [17], [18].

As computer vision evolved, vision-based vehicle control systems have been actively studied for autonomous driving cars. For example, lane keeping control system have been developed [19], [20] and lane lateral distance measurement methods have been also proposed [21], [22]. Vehicle body slip angle estimation based on vision systems have also been proposed [23]. Recently, vision-based lateral position and heading angle estimation with uneven time delay measurement has been studied [24].

In this paper, we aim to develop simultaneous vehicle lateral state and nonlinear tire force model estimation algorithms for autonomous driving cars. Since autonomous driving cars typically have on-board camera sensors, we first rewrite vehicle lateral dynamics in terms of lateral error variables with respect to the road which can be measured from the vision system. Neural network-based observers that can estimate system states and learn unknown system dynamics simultaneously have been previously proposed for certain mathematical classes of nonlinear systems [25] - [27]. Stability of the observers is guaranteed in the formulation. Recently, a new neural observer has been proposed based on a Lyapunov based nonlinear design technique in the conference paper [28]. Instead of the backpropagation approach, both the observer gains for state estimation and for weight adaptation are computed by solving a set of Linear inequality Matrix (LMI) conditions. In this paper, we utilize a neural network-based observer modified from the conference paper [28] to estimate both vehicle lateral states and the nonlinear tire model. We first show the performance of the proposed algorithm via MATLAB simulations with a low-order vehicle model and then validate the algorithm using an unknown high-order model from the commercial CarSim software.

II. Vehicle Dynamic Model

A bicycle model of the vehicle with two degrees of freedom (2-DOF) is considered to describe vehicle lateral dynamics, as shown in Fig. 1. The vehicle lateral translation y is defined along the body fixed lateral axis of the vehicle to the point O which is the instantaneous center of rotation of the vehicle. The vehicle yaw angle ψ is defined with respect to the global X axis. Using Newton's second law, the vehicle lateral dynamics are modeled with the following equations:

$$\begin{aligned} m(\ddot{y} + \dot{\psi}v_x) &= F_{yf} + F_{yr} \\ I_z\ddot{\psi} &= l_f F_{yf} - l_r F_{yr} \end{aligned} \tag{1}$$

where m is the total mass of the vehicle, I_z is the yaw moment of inertia of the vehicle, v_x is the longitudinal velocity of the vehicle at the center of gravity (c.g.), l_f and l_r are the distances from the c.g. to front and rear wheelbases, and F_{yf} and F_{yr} are the lateral tire forces on front and rear tires.

Experimental results show that the lateral tire force of a tire is a nonlinear function of slip angle and is linearly proportional

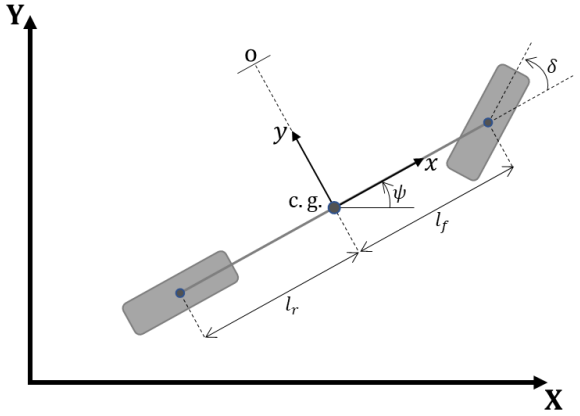

Fig. 1. 2-DOF bicycle model of the vehicle.

to the slip angle for small slip angles [29]. Based on this result, we write each of the front and rear tire forces as combination of a linear tire force model and an unknown nonlinear tire force model:

$$\begin{aligned} F_{yf} &= 2C_f\alpha_f + f_{yf}(\alpha_f) \\ F_{yr} &= 2C_r\alpha_r + f_{yr}(\alpha_r) \end{aligned} \tag{2}$$

where C_f and C_r are the cornering stiffnesses of each front and rear tire, α_f and α_r are the slip angles of front and rear wheels, and $f_{yf}(\alpha_f)$ and $f_{yr}(\alpha_r)$ are the unknown nonlinear front and rear tire force models, respectively.

Slip angles can be obtained from the following relations:

$$\begin{aligned} \alpha_f &= \delta - \frac{\dot{y} + l_f\dot{\psi}}{v_x} \\ \alpha_r &= -\frac{\dot{y} - l_r\dot{\psi}}{v_x} \end{aligned} \tag{3}$$

where δ is the steering angle of the front wheel of the vehicle.

Since we aim to develop algorithms to estimate both vehicle states and tire force model for autonomous driving cars, we rewrite the vehicle lateral dynamic model in terms of position and orientation error with respect to the road: lateral position error from center of lane e_1 and orientation error of vehicle with respect to the road e_2. Consider a vehicle traveling with constant longitudinal velocity v_x on a road with instantaneous radius R. Then, the desired yaw rate of the vehicle can be defined as

$$\dot{\psi}_{des} = \frac{v_x}{R}. \tag{4}$$

The following relations can be obtained for the position and orientation error variables [1]:

$$\begin{aligned} \dot{e}_1 &= \dot{y} + v_x(\psi - \psi_{des}) \\ \dot{e}_2 &= \dot{\psi} - \dot{\psi}_{des} \end{aligned}. \tag{5}$$

Using (2) and (5), we rewrite the lateral dynamic model (1) as

$$\begin{aligned} \ddot{e}_1 &= \left(\frac{-2C_f - 2C_r}{mv_x}\right)\dot{e}_1 + \left(\frac{2C_f + 2C_r}{m}\right)e_2 + \left(\frac{-2C_f l_f + 2C_r l_r}{mv_x}\right)\dot{e}_2 \\ &\quad + \frac{2C_f}{m}\delta + \left(\frac{-2C_f l_f + 2C_r l_r}{mv_x} - v_x\right)\dot{\psi}_{des} + \frac{f_{yf}(\alpha_f) + f_{yr}(\alpha_r)}{m} \\ \ddot{e}_2 &= \left(\frac{-2C_f l_f + 2C_r l_r}{I_z v_x}\right)\dot{e}_1 + \left(\frac{2C_f l_f - 2C_r l_r}{I_z}\right)e_2 + \left(\frac{-2C_f l_f^2 - 2C_r l_r^2}{I_z v_x}\right)\dot{e}_2 \\ &\quad + \left(\frac{-2C_f l_f^2 - 2C_r l_r^2}{I_z v_x}\right)\dot{\psi}_{des} - \ddot{\psi}_{des} + \frac{l_f f_{yf}(\alpha_f) - l_r f_{yr}(\alpha_r)}{I_z}. \end{aligned} \tag{6}$$

Assume that the lateral position error from center of lane and

orientation error of vehicle with respect to the road can be measured by vision system. Then, the state space model of the system with a state vector $\xi = [e_1 \quad \dot{e}_1 \quad e_2 \quad \dot{e}_2]^T$ is given by

$$\begin{aligned} \dot{\xi} &= A\xi + B_1\delta + B_2\dot{\psi}_{des} + B_3\ddot{\psi}_{des} + Ff \\ z &= C\xi \end{aligned} \tag{7}$$

where

$$A = \begin{bmatrix} 0 & 1 & 0 & 0 \\ 0 & \frac{-2C_f-2C_r}{mv_x} & \frac{2C_f+2C_r}{m} & \frac{-2C_fl_f+2C_rl_r}{mv_x} \\ 0 & 0 & 0 & 1 \\ 0 & \frac{-2C_fl_f+2C_rl_r}{I_zv_x} & \frac{2C_fl_f-2C_rl_r}{I_z} & \frac{-2C_fl_f^2-2C_rl_r^2}{I_zv_x} \end{bmatrix},$$

$$B_1 = \begin{bmatrix} 0 \\ \frac{2C_f}{m} \\ 0 \\ \frac{2C_fl_f}{I_z} \end{bmatrix}, \quad B_2 = \begin{bmatrix} 0 \\ \frac{-2C_fl_f+2C_rl_r}{mv_x} - v_x \\ 0 \\ \frac{-2C_fl_f^2-2C_rl_r^2}{I_zv_x} \end{bmatrix}, \quad B_3 = \begin{bmatrix} 0 \\ 0 \\ 0 \\ -1 \end{bmatrix}, \tag{8}$$

$$F = \begin{bmatrix} 0 & 0 \\ \frac{1}{m} & \frac{1}{m} \\ 0 & 0 \\ \frac{l_f}{I_z} & -\frac{l_r}{I_z} \end{bmatrix}, \quad f = \begin{bmatrix} f_{yf}(\alpha_f) \\ f_{yr}(\alpha_r) \end{bmatrix}, \quad C = \begin{bmatrix} 1 & 0 & 0 & 0 \\ 0 & 0 & 1 & 0 \end{bmatrix}.$$

Therefore, we develop an algorithm to estimate the state variables and the unknown nonlinear tire force using the above nonlinear vehicle model. Note that the above model derivation differs from standard textbook representations [1] where the road radius and hence $\dot{\psi}_{des}$ are assumed constant.

III. Vehicle Lateral States and Nonlinear Tire Model Estimation

A data-driven approach is proposed to estimate the nonlinear tire force model and vehicle states. First, we consider a neural approximator to deal with the unknown nonlinear tire force term. Then, a neural network-based observer with the neural approximator is utilized to estimate vehicle states and to learn the weights of the neural approximator.

A. Neural Approximator

Based on the capability of the neural network to approximate nonlinear functions [25], [30], the following approximator can be used to represent the nonlinear tire force term f:

$$f = \begin{Bmatrix} f_1 \\ f_2 \\ \vdots \\ f_r \end{Bmatrix} = \gamma \begin{Bmatrix} \vdots \\ \sum_{j=1}^{N} W_{ij}\sigma_{ij}(\xi,u) + \varepsilon_i(\xi,u) \\ \vdots \end{Bmatrix} \tag{9}$$

for $i = 1,2,\cdots,r$ where r is the number of nonlinear functions ($r = 2$ since there are two unknown nonlinear functions f_{yf} and f_{yr}), $\gamma = \mathrm{diag}(\gamma_1,\gamma_2,\cdots,\gamma_r)$ is a matrix to scale the neural approximator, N is the number of neurons utilized, W_{ij} is the adaptive weight in the output layer of the neural network which is unknown and is assumed to be constant, $\sigma_{ij}(\xi,u)$ is the activation function and is chosen by the designer, u is the input vector, and $\varepsilon_i(\xi,u)$ is the approximation error, which is bounded [30]. We assume the following conditions on the neural approximator:

1) The weights are bounded as

$$\left\|W_{ij}\right\|_\infty \le W_{max} \tag{10}$$

for all $i = 1,2,\cdots,r$ and $j = 1,2,\cdots,N$.

2) The activation functions are uniformly bounded as

$$-\infty < \underline{\sigma}_{ij} \le \sigma_{ij}(\xi,u) \le \overline{\sigma}_{ij} < \infty \tag{11}$$

and are differentiable Lipschitz continuous functions with a bounded Jacobian:

$$-\infty < a_{pq} \le \frac{\partial\sigma_{ij}}{\partial\xi_q}(\xi,u) \le b_{pq} < \infty \tag{12}$$

for every $\xi \in \mathbb{R}^n$, $i = 1,2,\cdots,r$ and $j = 1,2,\cdots,N$ where $p = j + N(i-1)$.

Front and rear slip angles can be computed from the estimated states and inputs as

$$\begin{aligned} \hat{\alpha}_f &= \delta + \frac{-\dot{\hat{e}}_1 + v_x\hat{e}_2 - l_f\dot{\hat{e}}_2}{v_x} - \frac{l_f\dot{\psi}_{des}}{v_x} \\ \hat{\alpha}_r &= \frac{-\dot{\hat{e}}_1 + v_x\hat{e}_2 + l_r\dot{\hat{e}}_2}{v_x} + \frac{l_r\dot{\psi}_{des}}{v_x} \end{aligned}. \tag{13}$$

Then, the estimated nonlinear tire force term can be written using the activation functions as functions of slip angles:

$$\hat{f} = \gamma \begin{Bmatrix} \sum_{j=1}^{N} \widehat{W}_{1j}\sigma_{1j}(\hat{\alpha}_f) \\ \sum_{j=1}^{N} \widehat{W}_{2j}\sigma_{2j}(\hat{\alpha}_r) \end{Bmatrix}. \tag{14}$$

B. Neuro-Adaptive Observer

Using the neural approximator (14), a neural network-based observer is utilized to estimate vehicle states and to learn the weights of the neural approximator:

$$\begin{aligned} \dot{\hat{\xi}} = A\hat{\xi} + L(z - C\hat{\xi}) + B_1\delta + B_2\dot{\psi}_{des} + B_3\ddot{\psi}_{des} + \\ F\gamma \begin{Bmatrix} \vdots \\ \sum_{j=1}^{N} \widehat{W}_{ij}\sigma_{ij}(\hat{\alpha}_f,\hat{\alpha}_r) \\ \vdots \end{Bmatrix} \\ \dot{\widehat{W}}_{ij} = \mathrm{K}_{ij}(z - C\hat{\xi}) \end{aligned} \tag{15}$$

for $i = 1,2,\cdots,r$ where L and K_{ij} are observer gain matrices to be computed.

Let the state estimation error be $\tilde{\xi} = \xi - \hat{\xi}$, and suppose the neural approximator can model the unknown nonlinear functions with ideal weights, i.e., $\varepsilon_i(\xi,u) \cong 0$. Then, using (7), (9) and (15), the state estimation error dynamics are derived as

$$\dot{\tilde{\xi}} = (A - LC)\tilde{\xi} + F\gamma \begin{Bmatrix} \vdots \\ \sum_{j=1}^{N} \widetilde{W}_{ij}\sigma_{ij} \\ \vdots \end{Bmatrix} + F\gamma \begin{Bmatrix} \vdots \\ \sum_{j=1}^{N} \widehat{W}_{ij}\tilde{\sigma}_{ij} \\ \vdots \end{Bmatrix} \tag{16}$$

for $i = 1,2,\cdots,r$ where $\widetilde{W}_{ij} = W_{ij} - \widehat{W}_{ij}$, $\sigma_{ij} = \sigma_{ij}(\alpha_f,\alpha_r)$, $\hat{\sigma}_{ij} = \sigma_{ij}(\hat{\alpha}_f,\hat{\alpha}_r)$ and $\tilde{\sigma}_{ij} = \sigma_{ij} - \hat{\sigma}_{ij}$. We define w as the column-wise vectorization of W_{ij}:

$$w = [W_{11},W_{12},\cdots,W_{1N},\cdots,W_{r1},W_{r2},\cdots,W_{rN}]^T \tag{17}$$

Let the parameter estimation error be $\tilde{w} = w - \hat{w}$. As a result, the parameter estimation error dynamics can be written as

$$\dot{\tilde{w}} = -KC\tilde{\xi} \tag{18}$$

where $K = [\mathrm{K}_{11},\mathrm{K}_{12},\cdots,\mathrm{K}_{1N},\cdots,\mathrm{K}_{r1},\mathrm{K}_{r2},\cdots,\mathrm{K}_{rN}]^T$. Using the following notations

$$\begin{aligned} \Phi(\sigma) &= \mathrm{diag}(\sigma_{11},\sigma_{12},\cdots,\sigma_{1N},\cdots,\sigma_{r1},\sigma_{r2},\cdots,\sigma_{rN}) \\ \widehat{\Omega} &= \mathrm{diag}(\widehat{W}_{11},\widehat{W}_{12},\cdots,\widehat{W}_{1N},\cdots,\widehat{W}_{r1},\widehat{W}_{r2},\cdots,\widehat{W}_{rN}) \\ \tilde{\varsigma} &= [\tilde{\sigma}_{11},\tilde{\sigma}_{12},\cdots,\tilde{\sigma}_{1N},\cdots,\tilde{\sigma}_{r1},\tilde{\sigma}_{r2},\cdots,\tilde{\sigma}_{rN}]^T \end{aligned} \tag{19}$$

and $\Gamma = \gamma \otimes 1_N^T$ (1_N is a column vector of N elements all set to one, and $\otimes$ denotes the Kronecker product), the state estimation

error dynamics (16) can be represented in the compact form as

$$\dot{\tilde{\xi}} = (A - LC)\tilde{\xi} + G\Phi(\sigma)\tilde{w} + G\hat{\Omega}\tilde{\varsigma} \tag{20}$$

where $G = F\Gamma$. By introducing an augmented state vector

$$\tilde{e} = [\tilde{\xi} \quad \tilde{w}]^T \tag{21}$$

the estimation error dynamics become

$$\dot{\tilde{e}} = (A_e(\sigma) - L_e C_e)\tilde{e} + G_e\hat{\Omega}\tilde{\varsigma} \tag{22}$$

where

$$A_e(\sigma) = \begin{bmatrix} A & G\Phi(\sigma) \\ 0 & 0 \end{bmatrix}, \quad L_e = \begin{bmatrix} L \\ K \end{bmatrix}, \quad G_e = \begin{bmatrix} G \\ 0 \end{bmatrix}, \quad C_e = [C \quad 0] \tag{23}$$

We can compute the observer gains by solving the following set of LMIs that is constructed to ensure stability of the estimation error dynamics (22).

Theorem 1. If there exist matrices $P = P^T > 0$, and R of appropriate dimensions, and fixed scalars $\alpha > 0$ and $\kappa > 0$ such that

$$\begin{bmatrix} \Xi & PG_e(W_{max}I) \\ (W_{max}I)^T G_e^T P & -\dfrac{\kappa}{\kappa+1}I \end{bmatrix} \leq 0, \quad \forall\sigma \in \Delta_0 \tag{24}$$

where

$$\begin{aligned} \Xi &= A_e(\sigma)^T P + PA_e(\sigma) - C_e^T R^T - RC_e \\ &\quad + (1+\kappa)\mathcal{N}\mathcal{N}^T - \mathcal{M} + 2\alpha P \\ \mathcal{M} &= \begin{bmatrix} \frac{1}{2}(\mathcal{H}_1^T\mathcal{H}_2 + \mathcal{H}_2^T\mathcal{H}_1) & 0 \\ 0 & 0 \end{bmatrix} \\ \mathcal{N} &= \begin{bmatrix} -\frac{1}{2}(\mathcal{H}_1^T + \mathcal{H}_2^T) \\ 0 \end{bmatrix} \\ \mathcal{H}_1 &= \begin{bmatrix} a_{11}, a_{12}, \cdots, a_{1n} \\ a_{21}, a_{22}, \cdots, a_{2n} \\ \vdots \\ a_{(rN)1}, a_{(rN)2}, \cdots, a_{(rN)n} \end{bmatrix} \\ \mathcal{H}_2 &= \begin{bmatrix} b_{11}, b_{12}, \cdots, b_{1n} \\ b_{21}, b_{22}, \cdots, b_{2n} \\ \vdots \\ b_{(rN)1}, b_{(rN)2}, \cdots, b_{(rN)n} \end{bmatrix} \end{aligned} \tag{25}$$

and

$$\begin{aligned} \Delta_0 = \{\sigma = (\sigma_{11}, \cdots, \sigma_{rN}) | \sigma_{ij} \in \{\underline{\sigma}_{ij}, \overline{\sigma}_{ij}\}, \\ i = 1, \cdots, r \text{ and } j = 1, \cdots, N\} \end{aligned} \tag{26}$$

Then the estimation error dynamics (22) with observer gain

$$L_e = P^{-1}R \tag{27}$$

is exponentially stable with a minimum convergence rate of α.

Proof. Theorem 1 is constructed by modification of the results in the previous conference paper [28]. The plant model used in this journal paper is slightly different from the conference paper and more applicable to real world systems (It does not require a constant term involving the neural weights in the plant dynamic equations). But the philosophy used in the derivation of the proof remains the same. The Lyapunov function candidate $V = \tilde{e}^T P\tilde{e}$ is considered to analyze the stability and then the condition $\dot{V} + 2\alpha V \leq 0$ is applied for exponential stability to obtain the LMI (24). Due to the strict 8-page limit of this paper, we omit the proof and instead cite the conference paper [28].

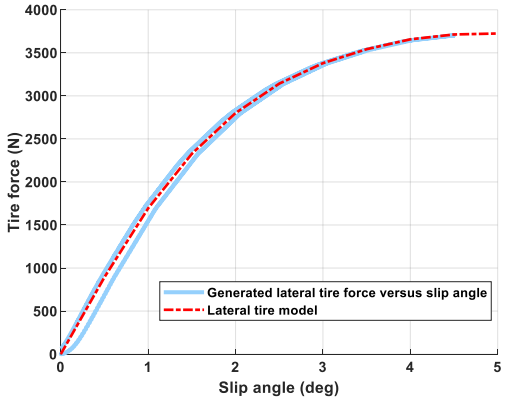

Fig. 2. Comparison between the generated lateral tire force from a lane change maneuver and the lateral tire force model in CarSim simulation.

C. Lateral Tire Model Estimation

In this section, a practical problem associated with convergence of the neural network weights will be discussed, and a least squares-based algorithm proposed to deal with obtaining better initial conditions for convergence.

First, the developed lateral dynamic model (7) is from a 2-DOF bicycle model and assumes that the tire force depends on only lateral slip angle variable in (2). However, the actual lateral tire force in CarSim can be quite different from the tire force computed from only the simple lateral tire model. Fig. 2 shows a result from CarSim simulation during a vehicle lane change maneuver. As shown in Fig. 2, the generated lateral tire force versus its slip angle includes hysteresis and does not match the simple lateral tire model. The mismatch is especially large when the car just starts its lateral motion due to tire lag.

Second, it turns out that the force estimates can converge to actual forces with different possible values of neural weights. The converged values of weights depend on the choice of initial conditions for the neural weights.

In order to obtain appropriate initial conditions for the neural weights, a simple algorithm based on a least squares method is proposed. The procedure is as follows:

Step 1: Store the data set of estimated values of $\hat{\sigma}$ and $\hat{f}$ obtained from the neuro-adaptive observer for every sample.

Step 2: Set $\hat{f}$ to zero when the slip angle is very small.

Step 3: Once a data set using a vehicle lateral maneuver is obtained, compute weights using a least squares method with regularization [31]:

$$\hat{w}^0 = \left(\begin{bmatrix} \Gamma\Phi^1(\hat{\sigma}) \\ \Gamma\Phi^2(\hat{\sigma}) \\ \vdots \\ \Gamma\Phi^s(\hat{\sigma}) \end{bmatrix}^T \begin{bmatrix} \Gamma\Phi^1(\hat{\sigma}) \\ \Gamma\Phi^2(\hat{\sigma}) \\ \vdots \\ \Gamma\Phi^s(\hat{\sigma}) \end{bmatrix} + \rho I \right)^{-1} \begin{bmatrix} \Gamma\Phi^1(\hat{\sigma}) \\ \Gamma\Phi^2(\hat{\sigma}) \\ \vdots \\ \Gamma\Phi^s(\hat{\sigma}) \end{bmatrix}^T \begin{bmatrix} \hat{f}^1 \\ \hat{f}^2 \\ \vdots \\ \hat{f}^s \end{bmatrix} \tag{28}$$

where ρ is a positive scalar, the superscript denotes each sample, and s is the number of samples.

Step 4: Update the weights in real-time using $\hat{w}^0$ as initial conditions to the observer.

We set upper bounds of both front and rear slip angles to be 0.5 degrees for this initialization so as to avoid tire force regions involving significant mismatch.

Finally, front and rear tire forces are calculated using the real-time value of the estimated weights $\widehat{W}_{ij}^*$:

$$F_{yf} = 2C_f\alpha_f + \gamma_1 \sum_{j=1}^{N} \widehat{W}_{1j}^* \sigma_{1j}(\alpha_f)$$
$$F_{yr} = 2C_r\alpha_r + \gamma_2 \sum_{j=1}^{N} \widehat{W}_{2j}^* \sigma_{2j}(\alpha_r) \quad (29)$$

It is found that no matter what the initial conditions of the weights are, the estimated tire forces do always match the actual forces well. However, using the least squares approach for initialization helps weights converge to global rather than locally optimum values.

IV. Simulation Results

In order to validate the proposed algorithm for vehicle state and lateral tire model estimation, we conduct simulation studies using MATLAB/Simulink and CarSim. The CARSIM software incorporates a high-order vehicle model that includes both lateral and longitudinal forces and further many other details of other vehicle motions, as well as coupled lateral and longitudinal tire forces. The vehicle model from CarSim chosen for the simulation studies is a D-Class sedan with default parameters ($m = 1529.95$ kg, $I_z = 4607.47$ kg-m^2, $l_f = 1.13906$ m, and $l_r = 1.63716$ m). A sampling time of 1 milli-second is utilized for all the CarSim simulations. Intricate details of the high-order CarSim model are unknown and are not utilized by the neuro-adaptive observer. The speed of the vehicle is controlled to a desired value using a PI controller and the desired speed is set to 30 m/s. Cornering and lane change maneuvers are considered in the simulation studies.

For the neuro-adaptive observer, 8 soft clipping functions are considered (4 activation functions are utilized for each front and rear tire force estimation). The activation functions for the front nonlinear tire model estimation are

$$\sigma_{1j}(\hat{\alpha}_f) = \hat{\alpha}_f + \frac{1}{\lambda}\log\frac{1+e^{-\lambda(\hat{\alpha}_f - \underline{\beta}_{1j})}}{1+e^{\lambda(\hat{\alpha}_f - \bar{\beta}_{1j})}} \quad (30)$$

for $j = 1,2,3,4$ where $\underline{\beta}_{11} = \underline{\beta}_{12} = \underline{\beta}_{13} = 0.005$, $\underline{\beta}_{14} = 0.1$, $\bar{\beta}_{11} = 0.02$, $\bar{\beta}_{12} = 0.05$, $\bar{\beta}_{13} = 0.08$, $\bar{\beta}_{14} = 0.1$, and $\lambda = 300$. The activation functions for the rear nonlinear tire model estimation are

$$\sigma_{2j}(\hat{\alpha}_r) = \hat{\alpha}_r + \frac{1}{\lambda}\log\frac{1+e^{-\lambda(\hat{\alpha}_r - \underline{\beta}_{2j})}}{1+e^{\lambda(\hat{\alpha}_r - \bar{\beta}_{2j})}} \quad (31)$$

for $j = 1,2,3,4$ where $\underline{\beta}_{21} = \underline{\beta}_{22} = \underline{\beta}_{23} = 0.005$, $\underline{\beta}_{24} = 0.1$, $\bar{\beta}_{21} = 0.01$, $\bar{\beta}_{22} = 0.03$, $\bar{\beta}_{23} = 0.08$, $\bar{\beta}_{24} = 0.1$, and $\lambda = 300$.

The values of $\underline{\beta}$ and $\bar{\beta}$ were selected to allow the activation functions to cover the operating range sufficiently well. One of the activation functions is set to be constant with equal lower and upper bounds, i.e., $\underline{\beta} = \bar{\beta}$ which helps the approximator to learn the obtained data by also allowing for a bias term. The parameter λ adjusts the corner sharpness of the function.

Observer gains are obtained by solving Theorem 1 with $\alpha = 2$, $\gamma = \mathrm{diag}(5000, 5000)$, $W_{max} = 50$, and $\kappa = 1$:

$$L = \begin{bmatrix} 7.4476 & 0.2230 \\ 35496.2923 & -1403.4068 \\ 0.2687 & 4.3756 \\ -1549.7253 & 15585.8620 \end{bmatrix} \times 10^3$$
$$K = \begin{bmatrix} 22907.6171 & 17507.4461 \\ 50297.2733 & 38508.3831 \\ 76176.5389 & 58477.9673 \\ 183230.2756 & 140010.5853 \\ 12668.9462 & -12684.5717 \\ 29281.1094 & -29328.7527 \\ 67379.8128 & -67667.3821 \\ 169016.7685 & -169223.4162 \end{bmatrix} \times 10^4 \quad (32)$$

The initial conditions of the system and observer are set to zero. In each simulation study, the initial values of the weights of the neural approximator are obtained by using the least squares-based algorithm described earlier.

In this paper, 3 simulation studies will be presented:

- *Study 1*: MATLAB simulation with a low order vehicle model based on known cornering stiffness
- *Study 2*: CarSim simulation with a high order vehicle model based on unknown cornering stiffness
- *Study 3*: CarSim simulation with a high order vehicle model in the present of sensor measurement noise

A. MATLAB Simulation with Low Order Vehicle Model

Using MATLAB simulations with the low order vehicle model described in section II, we first validate the proposed algorithm with no higher order model uncertainty. A cornering maneuver is considered - The vehicle is traveling on a road that is initially straight and then becomes circular with a radius first of 300 meters and then 250 meters. The desired path for the road is shown in Fig. 3. Also, we assume that the vehicle is controlled by a feedback steering controller and Fig. 3 shows

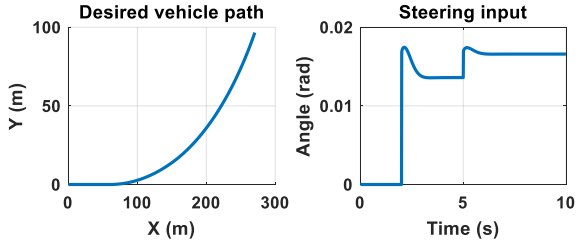

Fig. 3. Low order vehicle model simulation results: desired vehicle path for cornering maneuver, and steering input.

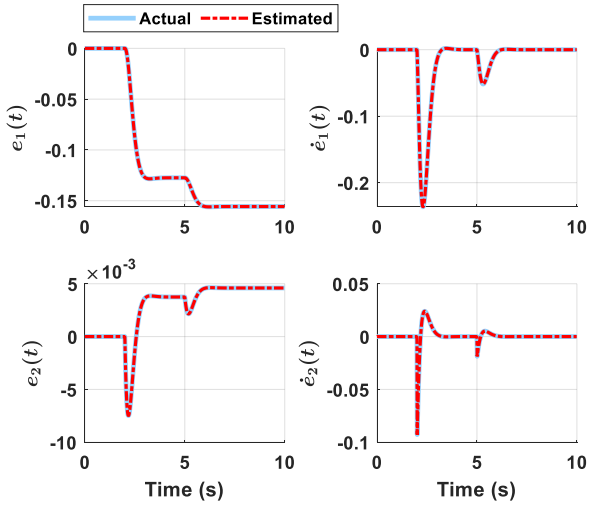

Fig. 4. Low order vehicle model simulation results: estimation of vehicle state variables.

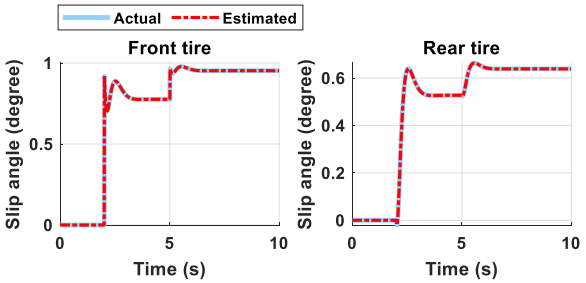

Fig. 5. Low order vehicle model simulation results: front and rear slip angle estimation.

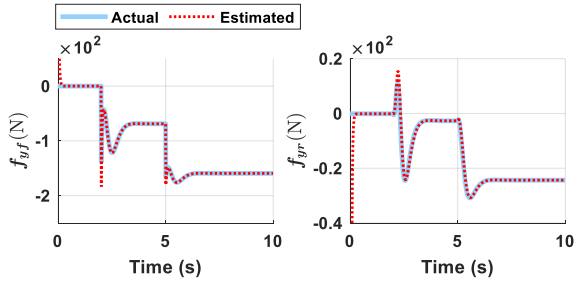

Fig. 6. Low order vehicle model simulation results: tire force estimation (nonlinear portion of tire force model).

the steering input to follow the desired vehicle path. The value of both front and rear tire cornering stiffness is 102466.1678 N/rad and is assumed to be known.

As shown in Fig. 4, the observer provides very good performance on the vehicle state estimation. As a result, the slip angles are accurately estimated by using (13), as shown in Fig. 5. Also, Fig. 6 shows the results of the nonlinear tire force estimation and the error is seen to be very small. Fig. 7(a) and 7(b) show the weight estimation. Weight adaptation can be seen in the zoomed-in plots of Fig. 7(b). Finally, Fig. 8 shows the tire model estimation result. The estimated lateral tire model is seen to match the real values accurately over the range of slip angles excited by the simulations.

B. CarSim Simulation under Unknown Cornering Stiffness

The proposed algorithm is also validated via simulations using the CarSim software containing a high order vehicle model. Significant model mismatch exists since the observer is based on just a simple bicycle model. So far, we have assumed that the cornering stiffness for the linear portion of the tire model is known. Next, we show that the proposed method can estimate both vehicle states and the lateral tire model without knowing the actual cornering stiffness. We assume that the value of both front and rear tire cornering stiffnesses is 102466.1678 N/rad. However, the actual cornering stiffness of the front and rear tires are set to be 90211.1436 N/rad and 87945.9970 N/rad, respectively. Lane change maneuvers are considered to learn the CarSim tire model over an adequately large range of slip angle. Fig. 9 shows the desired vehicle path and the steering input to conduct the lane change maneuvers.

Since the unknown nonlinear function estimation compensates for the linear term error due to the incorrect cornering stiffness, the vehicle states and slip angles can be correctly estimated, as shown in Fig. 10 and 11. Due to the linear term compensation, the nonlinear tire force terms do not match, as shown in Fig. 12. However, the total lateral tire model

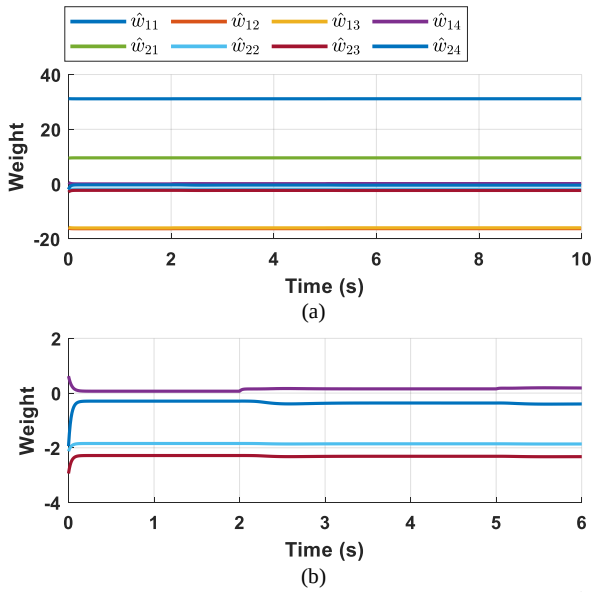

Fig. 7. Low order vehicle model simulation results: estimation of neural weights. (a) All neural weights. (b) Enlarged view of $\hat{w}_{14}$, $\hat{w}_{22}$, $\hat{w}_{23}$, and $\hat{w}_{24}$.

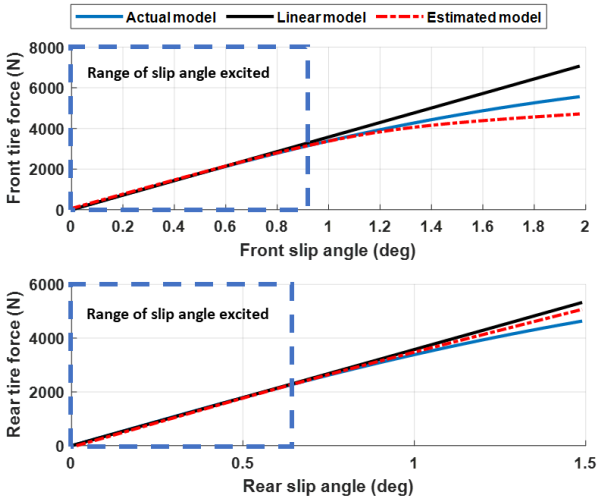

Fig. 8. Low order vehicle model simulation results: tire force model estimation (dotted blue box presents the range of slip angle excited).

can be obtained successfully by using (29) as shown in Fig. 14 because the tire model is defined as the combination of the linear tire model and the unknown nonlinear tire model in (2). Furthermore, we can correctly find the cornering stiffness from the estimated tire model: $\hat{C}_f = 89770.6981$ N/rad and $\hat{C}_r = 86991.2596$ N/rad.

C. CarSim Simulation under Sensor Noise

We validate the performance of the proposed algorithm in the presence of sensor noise on measurements. Random noise (uniformly distributed random signals with the interval $[-1cm, 1cm]$ and $[-1°, 1°]$) are added to both measurement channels. The value of both front and rear tire cornering stiffness is 102466.1678 N/rad and is assumed to be known. Lane change maneuvers are considered, as shown in Fig 15.

As seen in Fig. 16 and 17, both vehicle states and slip angles are estimated successfully in the presence of sensor noise. Also, Fig. 18 shows the results of the nonlinear tire force estimation. We can see that the neuro-adaptive observer provides good

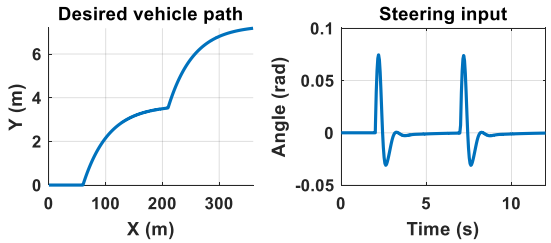

Fig. 9. CarSim simulation results (unknown cornering stiffness): desired vehicle path for lane change maneuvers, and steering input.

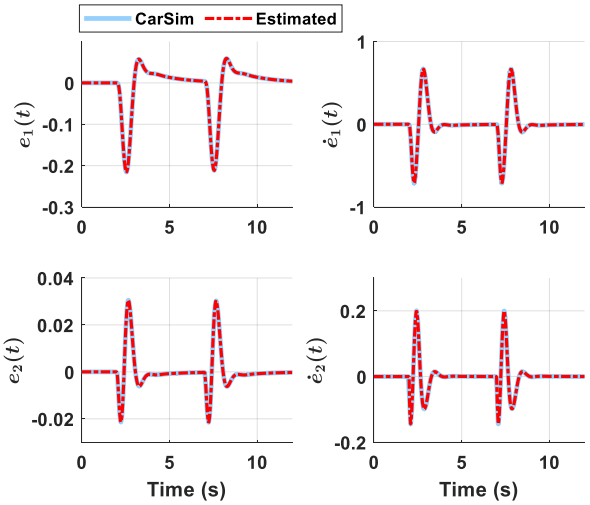

Fig. 10. CarSim simulation results (unknown cornering stiffness): estimation of vehicle state variables.

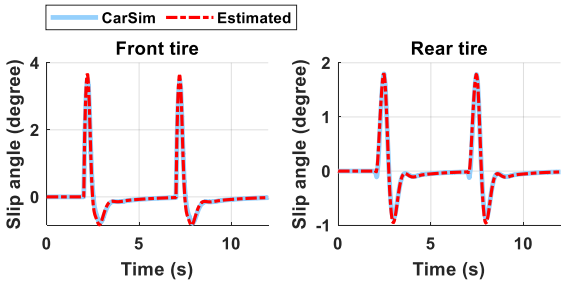

Fig. 11. CarSim simulation results (unknown cornering stiffness): front and rear slip angle estimation.

estimation results in spite of the measurement noise.

V. Conclusion

This paper developed a neuro-adaptive observer that can estimate both the real-time tire model as well as the states of an autonomously steered vehicle. The paper included formulation of the dynamic model in terms of lateral error variables with respect to the road and of the estimation problem, and design of the observer gains using LMIs. Simulations using both a low-order vehicle model and a high-order unknown model from the commercial software CarSim were conducted with lateral maneuvers including cornering and lane change maneuvers. Simulation studies demonstrated that the developed observer works very well and estimates both states and tire forces accurately. The importance of the developed neuro-adaptive method is that it can enable a new approach to obtaining tire models that are otherwise very difficult to identify in practice.

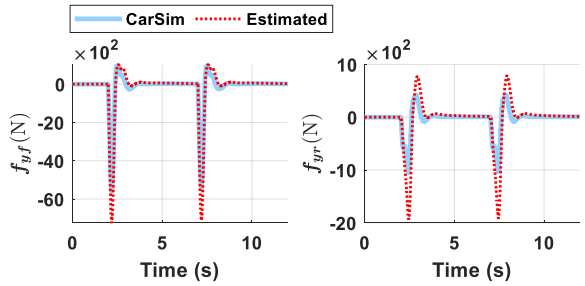

Fig. 12. CarSim simulation results (unknown cornering stiffness): tire force estimation (nonlinear portion of tire force model).

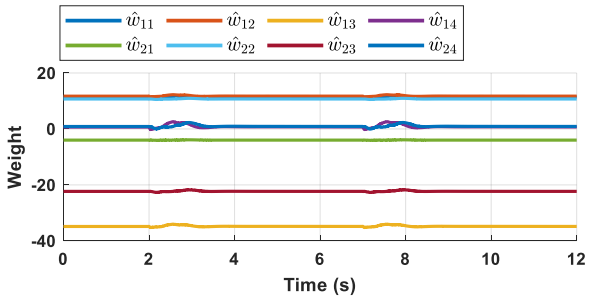

Fig. 13. CarSim simulation results (unknown cornering stiffness): estimation of neural weights.

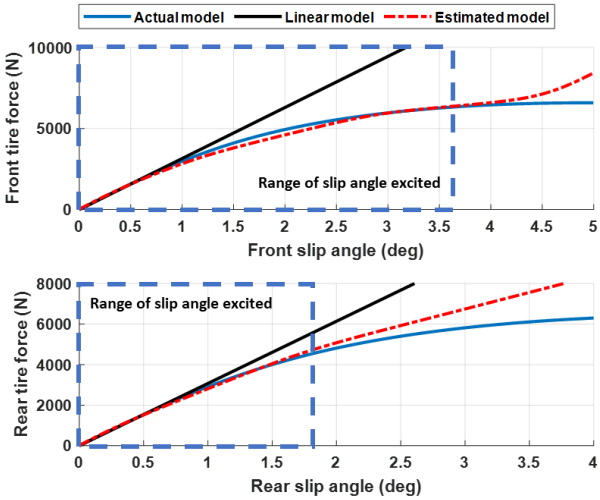

Fig. 14. CarSim simulation results (unknown cornering stiffness): tire model estimation (dotted blue box presents the range of slip angles excited).

References

[1] R. Rajamani, *Vehicle Dynamics and Control*. New York, NY, USA, ISBN 978-1-4614-1432-2, Springer, 2011.

[2] J. Farrelly and P. Wellstead, "Estimation of vehicle lateral velocity," Proceeding of *the 1996 IEEE International Conference on Control Applications*, Dearborn, MI, USA, 1996, pp. 552-557.

[3] A. Nguyen, T. Guerra, C. Sentouh and H. Zhang, "Unknown Input Observers for Simultaneous Estimation of Vehicle Dynamics and Driver Torque: Theoretical Design and Hardware Experiments," in *IEEE/ASME Transactions on Mechatronics*, vol. 24, no. 6, pp. 2508-2518, Dec. 2019.

[4] Y. J. Hsu, S. M. Laws and J. C. Gerdes, "Estimation of Tire Slip Angle and Friction Limits Using Steering Torque," in *IEEE Transactions on Control Systems Technology*, vol. 18, no. 4, pp. 896-907, July 2010.

[5] G. Phanomchoeng, R. Rajamani and D. Piyabongkarn, "Nonlinear Observer for Bounded Jacobian Systems, With Applications to Automotive Slip Angle Estimation," in *IEEE Transactions on Automatic Control*, vol. 56, no. 5, pp. 1163-1170, May 2011

[6] J. Dakhlallah, S. Glaser, S. Mammar and Y. Sebsadji, "Tire-road Forces Estimation Using extended Kalman Filter and Sideslip Angle Evaluation," *2008 American Control Conference*, Seattle, WA, 2008, pp. 4597-4602.

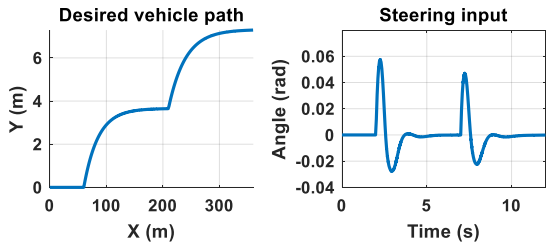

Fig. 15. CarSim simulation results (with sensor noise): desired vehicle path for lane change maneuvers, and steering input.

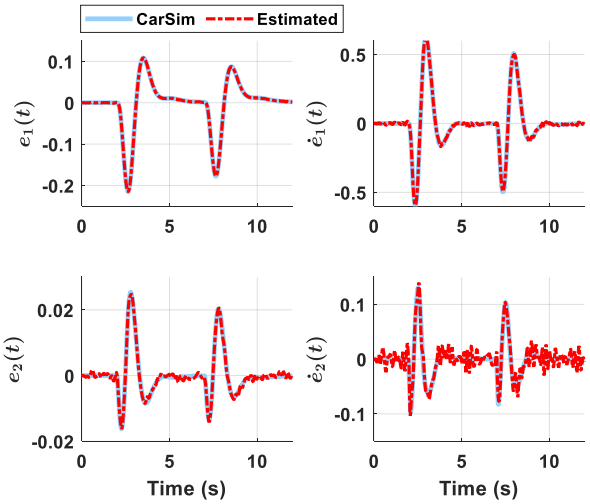

Fig. 16. CarSim simulation results (with sensor noise): estimation of vehicle state variables.

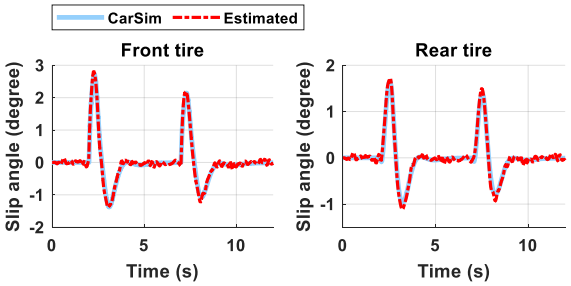

Fig. 17. CarSim simulation results (with sensor noise): front and rear slip angle estimation.

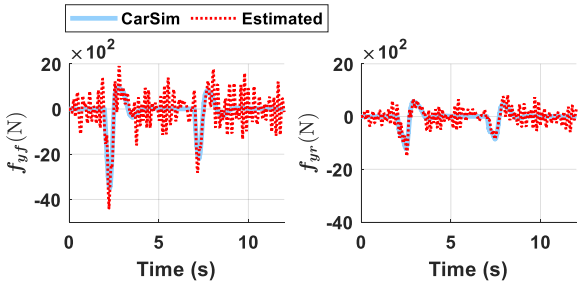

Fig. 18. CarSim simulation results (with sensor noise): tire force estimation (nonlinear portion of tire force model).

[7] S. Han and K. Huh, "Monitoring System Design for Lateral Vehicle Motion," in *IEEE Transactions on Vehicular Technology*, vol. 60, no. 4, pp. 1394-1403, May 2011.

[8] S. Antonov, A. Fehn and A. Kugi, "Unscented Kalman filter for vehicle state estimation," *Vehicle System Dynamics*, vol. 49, iss. 9, pp. 1497-1520, 2011.

[9] B. Zhang, H. Du, J. Lam, N. Zhang and W. Li, "A Novel Observer Design for Simultaneous Estimation of Vehicle Steering Angle and Sideslip Angle," in *IEEE Transactions on Industrial Electronics*, vol. 63, no. 7, pp. 4357-4366, July 2016.

[10] M. Doumiati, A. C. Victorino, A. Charara and D. Lechner, "Onboard Real-Time Estimation of Vehicle Lateral Tire–Road Forces and Sideslip Angle," in *IEEE/ASME Transactions on Mechatronics*, vol. 16, no. 4, pp. 601-614, Aug. 2011.

[11] M. Gadola, D. Chindamo, M. Romano and F. Padula, "Development and validation of a Kalman filter-based model for vehicle slip angle estimation," *Vehicle System Dynamics*, vol. 52 iss. 1, pp. 68-84, 2014.

[12] S. Cheng, L. Li and J. Chen, "Fusion Algorithm Design Based on Adaptive SCKF and Integral Correction for Side-Slip Angle Observation," in *IEEE Transactions on Industrial Electronics*, vol. 65, no. 7, pp. 5754-5763, July 2018.

[13] D. M. Bevly, J. Ryu and J. C. Gerdes, "Integrating INS Sensors With GPS Measurements for Continuous Estimation of Vehicle Sideslip, Roll, and Tire Cornering Stiffness," in *IEEE Transactions on Intelligent Transportation Systems*, vol. 7, no. 4, pp. 483-493, Dec. 2006.

[14] G. Baffet, A. Charara and J. Stephant, "Sideslip angle, lateral tire force and road friction estimation in simulations and experiments," *2006 IEEE International Conference on Control Applications*, Munich, 2006, pp. 903-908.

[15] F. Cheli, E. Sabbioni, M. Pesce and S. Melzi, "A methodology for vehicle sideslip angle identification: comparison with experimental data," *Vehicle System Dynamics*, vol. 45 iss. 6, pp. 549-563, 2007.

[16] K. Berntorp and S. Di Cairano, "Tire-Stiffness and Vehicle-State Estimation Based on Noise-Adaptive Particle Filtering," in *IEEE Transactions on Control Systems Technology*, vol. 27, no. 3, pp. 1100-1114, May 2019.

[17] C, Lundquist, and T. B. Schön, "Recursive identification of cornering stiffness parameters for an enhanced single track model." *IFAC Proceedings Volumes* 42.10 (2009): 1726-1731.

[18] F. Naets, S. van Aalst, B. Boulkroune, N. E. Ghouti and W. Desmet, "Design and Experimental Validation of a Stable Two-Stage Estimator for Automotive Sideslip Angle and Tire Parameters," in *IEEE Transactions on Vehicular Technology*, vol. 66, no. 11, pp. 9727-9742, Nov. 2017.

[19] V. Cerone, A. Chinu and D. Regruto, "Experimental results in vision-based lane keeping for highway vehicles," Proceedings of *the 2002 American Control Conference*, Anchorage, AK, USA, 2002, pp. 869-874 vol.2.

[20] J. Guo, J. Wang, Y. Luo and K. Li, "Takagi-Sugeno Fuzzy-based Robust H∞ Integrated Lane-Keeping and Direct Yaw Moment Controller of Unmanned Electric Vehicles," in *IEEE/ASME Transactions on Mechatronics*, doi: 10.1109/TMECH.2020.3032998.

[21] C. J. Taylor, J. Kosecka, R. Blasi, and J. Malik, "A Comparative Study of Vision-Based Lateral Control Strategies for Autonomous Highway Driving," *The International Journal of Robotics Research*, vol. 18, no. 5, pp. 442–453, 1999.

[22] J. Hsu, and M. Tomizuka, "Analyses of vision-based lateral control for automated highway system," *Vehicle system dynamics*, vol. 30, iss. 5, pp. 345-373, 1998.

[23] Yafei Wang, Binh Minh Nguyen, P. Kotchapansompote, H. Fujimoto and Y. Hori, "Vision-based vehicle body slip angle estimation with multi-rate Kalman filter considering time delay," *2012 IEEE International Symposium on Industrial Electronics*, Hangzhou, 2012, pp. 1506-1511.

[24] Y. Wang, Y. Liu, H. Fujimoto and Y. Hori, "Vision-Based Lateral State Estimation for Integrated Control of Automated Vehicles Considering Multirate and Unevenly Delayed Measurements," in *IEEE/ASME Transactions on Mechatronics*, vol. 23, no. 6, pp. 2619-2627, Dec. 2018.

[25] Y. H. Kim, F. L. Lewis, and C. T. Abdallah, "A dynamic recurrent neural-network-based adaptive observer for a class of nonlinear systems," *Automatica*, vol. 33, no. 8, pp. 1539–1543, 1997

[26] F. Abdollahi, H. Talebi, and R. Patel, "A Stable Neural Network-Based Observer With Application to Flexible-Joint Manipulators," *IEEE Transactions on Neural Networks*, vol. 17, no. 1, pp. 118–129, Jan 2006.

[27] R. Rahimilarki, Z. Gao, A. Zhang, and R. J. Binns, "Robust neural network fault estimation approach for nonlinear dynamic systems with applications to wind turbine systems," *IEEE Transactions on Industrial Informatics*, vol. 3203, no. c, pp. 1–1, 2019.

[28] A. Chakrabarty, A. Zemouche, R. Rajamani and M. Benosman, "Robust Data-Driven Neuro-Adaptive Observers With Lipschitz Activation Functions," *2019 IEEE 58th Conference on Decision and Control (CDC)*, Nice, France, 2019, pp. 2862-2867.

[29] P. B. Hans. *Tire and vehicle dynamics*. Elsevier, 2005.

[30] K. Hornik, "Approximation capabilities of multilayer feedforward networks," *Neural Networks*, vol. 4, no. 2, pp. 251–257, 1991.

[31] G. H. Golub, P. C. Hansen, and D. P. O'Leary. "Tikhonov regularization and total least squares." *SIAM journal on matrix analysis and applications*, vol. 21, no. 1, pp. 185-194, 1999.

Woongsun Jeon obtained his B.S. and M.S. degrees in mechanical engineering from Yonsei University, Seoul, Korea in 2010 and 2012, respectively, and the Ph.D. degree from the University of Minnesota in 2019. Currently he is a post-doctoral fellow at the University of Minnesota, Twin Cities, MN, USA. His research interests are in estimation, sensing, control theory and learning-based methods, including applications in intelligent transportation and robot systems.

Ankush Chakrabarty received a Ph.D. in Electrical and Computer Engineering at Purdue University as a Ross Fellow in 2016. Subsequently, he was a Postdoctoral Fellow at Harvard University where he developed control algorithms for a wearable artificial pancreas. He is currently a Research Scientist at Mitsubishi Electric Research Labs, where he works on machine learning and control engineering for applications including buildings, vehicles, and factory automation. He has published over 50 peer-reviewed articles and filed over 15 patents contributing to areas including machine learning for control, approximate nonlinear model predictive control, unknown input estimation, linear matrix inequalities, and embedded (wearable/implantable) medical devices. He is a Senior Member of the IEEE. He has an Erdös number of 4.

Ali Zemouche received his Ph.D. degree in automatic control in 2007, from the University Louis Pasteur, Strasbourg, France, where he held a post-doctorate position from October 2007 to August 2008. Dr. Zemouche has been an Associate Professor at the Centre de Recherche en Automatique de Nancy (CRAN UMR CNRS 7039) at the Université de Lorraine, since September 2008. His research activities include nonlinear systems, state observers, observer-based control, time-delay systems, robust control, learning-based methods, and application to real-world models. Dr. Zemouche is currently associate editor in international journals: *SIAM Journal of Control and Optimization*, *Automatica*, *IEEE Transactions on Automatic Control*, *European Journal of Control*, and *IEEE Systems Journal*. He is also a member of the Conference Editorial Board of IEEE Control Systems Society and IFAC TC2.3 (Non-Linear Control Systems).

Rajesh Rajamani obtained his M.S. and Ph.D. degrees from the University of California at Berkeley in 1991 and 1993 respectively and his B.Tech degree from the Indian Institute of Technology at Madras in 1989. Dr. Rajamani is currently the Benjamin Y.H. Liu-TSI Endowed Professor of Mechanical Engineering at the University of Minnesota. His active research interests include sensing and estimation for smart mechanical systems.

Dr. Rajamani has co-authored over 160 journal papers and is a co-inventor on 17 patent applications. He is the author of the popular book "Vehicle Dynamics and Control" published by Springer. Dr. Rajamani has served as Chair of the IEEE Technical Committee on Automotive Control and is currently Senior Editor of the *IEEE Transactions on Intelligent Transportation Systems*. He is a Fellow of ASME and has been a recipient of the CAREER award from the National Science Foundation, the Ralph Teetor Award from SAE, the O. Hugo Schuck Award from the American Automatic Control Council, and a number of best paper awards from conferences and journals. Several inventions from his laboratory have been commercialized through start-up ventures co-founded by industry executives. One of these companies, Innotronics, was recently recognized among the 35 Best University Start-Ups of 2016 by the US National Council of Entrepreneurial Tech Transfer.